# Isolinderalactone inhibits glioblastoma cell supernatant-induced angiogenesis

SEO-YEON LEE[1,2], JUNG HWA PARK[3,4], KANG-HYUN CHO[1,2], HUISEON KIM[1,2] and HWA KYOUNG SHIN[3,4]

Departments of [1]Pharmacology and [2]Biomedical Science, Wonkwang University School of Medicine, Iksan, Jeonbuk 54538; [3]Department of Korean Medical Science, School of Korean Medicine, Pusan National University; [4]Graduate Training Program of Korean Medicine for Healthy Aging, Pusan National University, Yangsan, Gyeongnam 50612, Republic of Korea

Received May 17, 2022; Accepted July 14, 2022

DOI: 10.3892/ol.2022.13448

**Abstract.** Glioblastoma multiforme (GBM) is the most frequently occurring malignant brain tumor in adults and is characterized by a high degree of vascularization. Glioblastoma cells communicate with their microenvironment and stimulate blood vessel formation to support tumor progression. It has previously been reported that isolinderalactone induces apoptosis in GBM cells and suppresses the growth of glioblastoma xenograft tumors *in vivo*. Furthermore, isolinderalactone has been shown to inhibit the hypoxia-driven upregulation of vascular endothelial growth factor (VEGF) in U-87 GBM cells and strongly reduce VEGF-triggered angiogenesis *in vitro* and *in vivo*. In the present study, the direct angiogenic effect of GBM and the effect of isolinderalactone on tumor angiogenesis were investigated. Culture supernatants were obtained from U-87 cells under normoxic or hypoxic conditions to provide normoxic conditioned medium (NCM) and hypoxic conditioned medium (HCM) respectively. The NCM and HCM were each used to treat to human brain microvascular endothelial cells (HBMECs), and their effects were observed using wounding migration and tube formation assays. HCM increased the migration and capillary-like tube formation of HBMECs when compared with NCM, and treatment with isolinderalactone suppressed the HCM-driven angiogenesis *in vitro*. Additionally, isolinderalactone decreased HCM-triggered angiogenic sprouting in HBMECs in a 3D microfluidic device after the application of an HCM-containing interstitial fluid flow. Furthermore, isolinderalactone strongly reduced HCM-triggered angiogenesis in an *in vivo* Matrigel plug assay in mice. These findings provide evidence of angiogenesis inhibition by isolinderalactone, and demonstrate the anti-angiogenic effect of isolinderalactone against the direct angiogenic effect of GBM tumor cells.

*Correspondence to:* Professor Seo-Yeon Lee, Department of Pharmacology, Wonkwang University School of Medicine, 460 Iksan-daero, Iksan, Jeonbuk 54538, Republic of Korea
E-mail: brainsw@gmail.com

Professor Hwa Kyoung Shin, Department of Korean Medical Science, School of Korean Medicine, Pusan National University, 49 Busandaehak-ro, Mulgeum-eup, Yangsan, Gyeongnam 50612, Republic of Korea
E-mail: julie@pusan.ac.kr

*Key words:* conditioned media, cytokine, endothelial cells, glioblastoma, hypoxia, microenvironment, paracrine, 3D microchip

## Introduction

Isolinderalactone is a sesquiterpene that may be isolated from extracts of *Lindera aggregata* root (1). The root extract of *Lindera aggregata*, commonly known as *Lindera*, has been used in traditional medicine to treat chest and abdominal pain and renal, cystic and rheumatic diseases (2). *Lindera* extract has also been used to treat diabetes and inflammation (3,4). Studies have demonstrated that isolinderalactone can inhibit tumor cell growth and induce apoptosis. For example, isolinderalactone has been shown to induce cell death in A549 non-small cell lung cancer cells by increasing p21 expression and regulating the Fas receptor/Fas ligand-mediated apoptosis pathway (5). In addition, isolinderalactone has been demonstrated to induce apoptosis in MDA-MB-231 breast cancer cells (6) and inhibit the migration and invasion of A549 lung cancer cells by inhibiting MMP-2 and β-catenin expression (7). Furthermore, our previous studies reported the ability of isolinderalactone to induce ovarian cancer cell death via the STAT3-mediated pathway (8) and inhibit glioblastoma growth and tumor angiogenesis (9,10).

Gliomas are the most frequently occurring primary malignant tumors of the brain. Glioblastoma multiforme (GBM) is the most aggressive brain tumor among gliomas and is characterized by high recurrence and mortality rates (11). The standard protocol for the treatment of GBM is maximal tumor resection in combination with radiotherapy and chemotherapy using the alkylating agent temozolomide (12,13). However, the prognosis of GBM patients is very poor, as the median survival time is only 14-18 months and the 5-year survival rate is <5% (13,14).

A significant feature of glioblastomas is a high degree of angiogenesis (11,15). GBM is associated with various types of neovascularization, including vasculogenesis, angiogenesis and intussusceptive microvascular growth (16). Tumor angiogenesis is the tumor-induced formation of new blood vessels from pre-existing blood vessels, and most solid tumors require sprouting angiogenesis for tumor progression (17). GBM vasculature shows structurally and functionally abnormal characteristics, such as changes in the association between endothelial cells and pericytes that lead to hyperpermeability and vessel leakage, and subsequently poor vessel perfusion and nutrient delivery (18,19). These vascular characteristics aggravate tumor hypoxia, and the secretion of hypoxia-mediated pro-angiogenic factors from inflammatory or tumor cells enhances vascular abnormalities.

Glioblastoma cells crosstalk with their microenvironment, and GBM can recruit healthy brain cells and create a tumor microenvironment to support tumor progression (20). GBM secretes cytokines such as vascular endothelial growth factor (VEGF), which stimulates the formation of blood vessels for tumor growth (21,22). VEGF is highly expressed in GBM and is associated with the grade of malignancy and the prognosis of patients with GBM (18,19). In our previous study, isolinderalactone suppressed the growth of glioblastoma xenograft tumors *in vivo* and induced apoptosis in U-87 GBM cells (9). In another of our previous studies, isolinderalactone was shown to inhibit hypoxia-stimulated VEGF expression in U-87 glioblastoma cells and strongly reduce VEGF-triggered angiogenesis *in vitro* and *in vivo* (10). In the present study, the direct angiogenic effect of GBM and the effect of isolinderalactone on GBM tumor-triggered angiogenesis were investigated. Tumor supernatants, specifically conditioned medium (CM) from U-87 cell culture, were used to trigger angiogenesis instead of VEGF. The CM was used to simulate a GBM tumor, and the ability of isolinderalactone to inhibit tumor cell supernatant-triggered angiogenesis *in vitro* and *in vivo* was investigated.

## Materials and methods

*Cell culture, hypoxic condition and reagents*. The human U-87 MG (ATCC HTB-14) cell line, which is derived from a glioblastoma of unknown origin, was purchased from the American Type Culture Collection. The U-87 MG cells were cultured at 37˚C in Dulbecco's modified Eagle's medium (DMEM; cat. no. 11965; Thermo Fisher Scientific, Inc.) supplemented with 10% fetal bovine serum (FBS; cat. no. 16000; Thermo Fisher Scientific, Inc.) and 1% penicillin/streptomycin (cat. no. 15140; Thermo Fisher Scientific, Inc.). Human brain microvascular endothelial cells (HBMECs; passages 7-9; ACBRI 376; Cell Systems) were cultured at 37˚C in Endothelial Cell Growth Medium-2 BulletKit™-microvascular (EGM-2-MV; CC-3202; Lonza Group, Ltd.). For the experiments under hypoxic conditions, cells were incubated at 37˚C in a hypoxic incubator (Forma™; cat. no. 3131; Thermo Fisher Scientific, Inc.) filled with 1% $O_2$, 5% $CO_2$ and balance $N_2$. Isolinderalactone (ALB-RS-6003) was obtained from ALB Technology, Ltd. and dissolved in dimethyl sulfoxide (DMSO; Duchefa Biochemie B.V.). Isolinderalctone was used to treat U-87 cells under hypoxia (2.5 or 5 $\mu$g/ml) and HBMECs were treated with HCM (2 $\mu$g/ml). Recombinant human basic fibroblast growth factor (BFGF; F0291) was purchased from Sigma-Aldrich. Recombinant human VEGF (293-VE) was purchased from R&D Systems, Inc. and reconstituted in phosphate-buffered saline (PBS) containing 0.1% bovine serum albumin (cat. no. 0332; VWR International, LLC.) according to the manufacturer's protocol.

*RNA extraction and reverse transcription-PCR (RT-PCR)*. Total RNA was isolated from U-87 cells using TRIzol® Reagent (cat. no. 15596; Thermo Fisher Scientific, Inc.). A PrimeScript™ 1st Strand cDNA Synthesis Kit (cat. no. 6110; Takara Bio, Inc.) was used to synthesize cDNA from 2 $\mu$g total RNA, according to the manufacturer's protocol. End-point PCR for the measurement of VEGF was performed using GAPDH as the reference gene for normalization with the following primers: VEGF (23) forward, 5'-GAGAATTCGGCCTCC GAAACCATGAACTTTCTGCT-3' (nucleotides plus *Eco*RI adapter) and reverse, 5'-GAGCATGCCCTCCTGCCCGGCT CACCGC-3' (nucleotides plus *Sph*I adapter) with a melting temperature of 65˚C for 30 cycles; and GAPDH forward, 5'-CGTGGAAGGACTCATGAC-3' and reverse, 5'-CAAATT CGTTGTCATACCAG-3' with a melting temperature of 55˚C for 27 cycles. The PCR products were mixed with Ezstain DNA loading dye (cat. no. B006M; Enzynomics, Inc.) and analyzed using a 1.2% agarose gel.

*Western blot assay*. U-87 cells were lysed using RIPA buffer (cat. no. 9806; Cell Signaling Technology, Inc.) supplemented with a protease inhibitor mixture (P3100; GenDEPOT) and a phosphatase inhibitor mixture (P3200; GenDEPOT). Total protein content was determined by Pierce™ BCA Protein Assay Kit (cat. no. #23225; Thermo Fisher Scientific, Inc.) according to the manufacturer's instructions. Total protein (20-30 $\mu$g/lane) was separated on 12% gels using SDS-PAGE and transferred onto a nitrocellulose membrane (Amersham; Cytiva). After transfer, the membrane was incubated with 5% skimmed milk (cat. no. #232100; Becton, Dickinson and Company) in PBS containing 0.1% Tween-20 (cat. no. TR1027-500-00; Biosesang) for 1 h at room temperature. The membrane was immunoblotted using an anti-VEGF antibody (1:1,000; sc-7269; Santa Cruz Biotechnology, Inc.) for 16 h at 4˚C. An α-tubulin antibody (1:3,000; T5168; Sigma-Aldrich; Merck KGaA), as the internal control, was incubated for 16 h at 4˚C. For the incubation with secondary antibody, HRP-conjugated anti-mouse antibody (1:10,000; #1031-05; SouthernBiotech) was applied for 1 h at room temperature. Chemiluminescence intensity was measured using an ImageQuant™ LAS 4000 apparatus (Cytiva). The quantification of band intensity was performed using ImageJ software (V1.8.0; National Institutes of Health) and normalized to the intensity of α-tubulin.

*Preparation of CM from glioblastoma cells*. The CM from normoxic U-87 cells (NCM) and the CM from hypoxic U-87 cells (HCM) were collected, concentrated and used in further experiments.

*In vitro angiogenesis assay*. U-87 cells were seeded at $1.5x10^6$ cells/100 mm dish and cultured for 2 days. The medium was replaced with EGM-2-MV (without VEGF and

bFGF) and incubated under normoxic or hypoxic conditions. After 16 h, CM was harvested, filtered using a Minisart® Syringe Filter (pore size 0.45 $\mu$m; Sartorius AG), concentrated twice (for wounding migration assay) or 10 times (for tube formation assay) with an Amicon® Ultra-15 Centrifugal Filter Unit (UFC901024; MilliporeSigma) and used to treat HBMECs.

*In vivo mouse Matrigel plug assay*. The U-87 cell medium was replaced with DMEM containing 0.5% FBS and incubated under normoxic or hypoxic conditions for 16 h. CM was collected, filtered using a Minisart Syringe Filter (pore size 0.45 $\mu$m), concentrated 100 times with an Amicon Ultra-15 Centrifugal Filter Unit and mixed with Matrigel (50 $\mu$l concentrated CM + 500 $\mu$l Matrigel).

*3D angiogenic sprouting assay*. U-87 cells cultured in DMEM containing 10% FBS were incubated under normoxic or hypoxic conditions for 16 h. CM was collected, filtered using a Minisart Syringe Filter (pore size 0.45 $\mu$m), and mixed with EGM-2-MV (without VEGF and bFGF) at a 2:1 ratio for use as interstitial fluid.

*In vitro angiogenesis assay: Wounding migration assay*. The migration assay was performed as described previously (24). Briefly, HBMECs were seeded into 60-mm culture dishes and incubated until they reached ~90% confluence. The monolayer was wounded with a razor and washed with an endothelial basal medium to remove cell debris, and the NCM (5 ml) or HCM (5 ml) from U-87 cells and 1 mM thymidine (T1895; Sigma-Aldrich) were added. The HCM-treated cells were incubated with or without isolinderalactone (2 $\mu$g/ml), and the cells were incubated for 16 h. The cells were then fixed, stained and imaged with an Olympus TH4-200 microscope (light microscope; Olympus Corporation). The migration activity was quantified by counting the number of cells that moved beyond the reference line.

*In vitro angiogenesis assay: Tube formation assay*. HBMECs ($3x10^4$ cells/well) were seeded onto polymerized Matrigel (cat. no. 354230; BD Biosciences) in a 24-well plate, and a tube formation assay was performed as previously described (24,25). HBMECs incubated with NCM (1 ml) or HCM (1 ml), the latter with or without 2 $\mu$g/ml isolinderalactone, were imaged with a TH4-200 microscope every hour for 10 h. Capillary-like tube networks were observed and the tube length and tube branching points (>3) were analyzed using iSolution full image analysis software (Image & Microscope Technology).

*3-Dimensional (3D) angiogenic sprouting assay in a microfluidic device*. 3D chips (DAX01) were purchased from AIM Biotech Pte. Ltd. and an angiogenic sprouting assay was performed as previously described (10). AIM connectors (LUC-1; AIM Biotech Pte. Ltd.) and a 1-cc syringe (Jung Rim Medical Industrial Co., Ltd.) were used to apply interstitial flow. Briefly, the central gel channel was filled with 2.5 mg/ml collagen gel solution (pH 7.4; 10 $\mu$l) prepared using Collagen I, rat tail (cat. no. 354236; Corning, Inc.), 10X PBS (cat. no. 70011-044; Thermo Fisher Scientific, Inc.) and 0.5 M NaOH (cat. no. 221465; Sigma-Aldrich), following the AIM Biotech protocol. The gel-filled device was polymerized for 30 min at 37˚C, the lateral media channels were hydrated using growth medium (EGM-2-MV, without VEGF or bFGF), and the devices were kept in a humidified $CO_2$ incubator until cell seeding. HBMECs were suspended in growth medium at a concentration of $1.5x10^6$ cells/ml, and the cell suspension (40 $\mu$l) was seeded onto one lateral channel of the 3D chip. After seeding the cells, the chips were tilted 90˚ to allow the cells to adhere to the gel surface and incubated at 37˚C for 15 min. The chips were then returned to their original orientation and incubated for 3 h. Then, the medium was replaced with fresh growth medium to remove any unattached cells. The next day, the AIM connectors and 1-cc syringe were connected. Subsequently, 200 $\mu$l growth medium was supplied to the cell seeding channel, and 1,000 $\mu$l of a mixture of NCM or HCM with growth medium and bFGF (10 ng/ml) was supplied to the medium channel. DMSO (0.1%) or isolinderalactone (2 $\mu$g/ml) was added to the medium channel containing the HCM mixture 6 days later. The medium was replaced daily, and sprouting was monitored using a TH4-200 phase-contrast microscope.

*Immunofluorescence staining and quantification of sprouting*. After 8 days of culture on the chip, immunofluorescence staining was performed according to the manufacturer's protocol. Briefly, HBMECs were washed, fixed with 4% paraformaldehyde for 15 min at room temperature, and permeabilized with 0.1% Triton X-100 for 30 min at room temperature. The cells were incubated with blocking buffer comprising 10% normal goat serum (S-1000; Vector Laboratories, Inc.) in 1X PBS for 2 h at room temperature, and then incubated with anti-VE-cadherin antibody (1:100 in 1X PBS; sc-9989; Santa Cruz Biotechnology, Inc.) overnight at 4˚C. The next day, the cells were washed with PBS and incubated with Alexa Fluor 488-conjugated secondary antibody (1:200; A-11001; Thermo Fisher Scientific, Inc.) and rhodamine-phalloidin for F-actin (5 U/ml; R415; Thermo Fisher Scientific, Inc.) for 1 h at room temperature. Nuclei were stained with DAPI (D1306; Molecular Probes; Thermo Fisher Scientific, Inc.). The z-stack images of angiogenic sprouting were captured using a Zeiss LSM 700 laser scanning confocal microscope (Carl Zeiss AG). The sprout diameter was analyzed using images captured from orthographic views of the middle of the sprouts, as previously reported (26). Sprout length was measured starting from the point at which the sprouts began to extend. All analyses were performed using iSolution full image analysis software.

*In vivo mouse Matrigel plug assay*. A total of 16 C57BL/6 mice (6-week-old males; 20-25 g) were purchased from Nara Biotechnology. The mice were housed under a 12-h light/dark cycle at 23±1˚C with 40-60% humidity and allowed *ad libitum* access to food and water. The mice were adapted to these conditions for at least 7 days prior to the experiments. The mice were maintained in accordance with the Pusan National University Guidelines for the Care and Use of Laboratory Animals and the experiments using the mice were approved by the Institutional Review Board of Pusan National University (PNU-2019-2361). Humane endpoints for euthanasia were considered to be the prolonged observation of a 40% reduction in food and water intake

and/or unstable breathing. The feeding and condition of the mice were assessed and monitored daily post-surgery for any signs of decreased activity and a reduction in food intake. However, no signs of these conditions were observed. The following groups were established: NCM (n=4), HCM + DMSO (n=6) and HCM + iso (n=6). Growth factor-reduced Matrigel (500 $\mu$l; cat. no. 354230) containing NCM or HCM (concentrated 100 times) was injected subcutaneously under anesthesia. The mice were anesthetized with isoflurane delivered using a face mask (3% for induction and 1.5% for maintenance, in 80% $N_2O$ and 20% $O_2$). The next day, the treatment of the mice in the HCM + iso group was initiated with an intraperitoneal injection of 5 mg/kg/day isolinderalactone for 6 days. The mice in the HCM + DMSO group were treated with DMSO at the same time points. On day 8, the mice were sacrificed by exposure to 70% carbon dioxide following deep anesthesia with 50 mg/kg sodium thiopental (IP), and the Matrigel plugs were harvested. The hemoglobin content of the Matrigel plugs was measured using a hemoglobin assay kit (MAK115; Sigma-Aldrich) to evaluate blood vessel formation.

*Statistical analysis*. All data are expressed as the mean ± standard error of the mean. The differences between groups were analyzed for statistical significance using one-way ANOVA followed by Tukey's post hoc test. P<0.05 was considered to indicate a statistically significant difference.

## Results

*Direct angiogenic effect of GBM CM is suppressed by isolinderalactone*. To examine the direct angiogenic effect of GBM, CM from U-87 tumor cells was used. The CM was obtained from U-87 cells under normoxic or hypoxic conditions. Before collecting the CM, western blotting and RT-PCR analyses confirmed that VEGF expression was stimulated in U-87 cells under hypoxic conditions (Fig. 1). Hypoxia significantly increased VEGF protein and mRNA levels in the U-87 cells compared with those in U-87 cells cultured under normoxic conditions, and these increases in VEGF levels were significantly decreased by treatment with isolinderalactone. Culture supernatants were obtained from normoxic and hypoxic U-87 cells and used to perform *in vitro* and *in vivo* assays (Fig. 2A).

First, whether HCM affects angiogenesis was investigated using *in vitro* angiogenesis assays, in which HCM was used to simulate the angiogenesis-stimulating effects of glioblastoma on neighboring endothelial cells. The effect of HCM on endothelial migration, a critical feature in the formation of new blood vessels, was evaluated (27). HCM significantly stimulated the migration of HBMECs, whereas isolinderalactone treatment significantly attenuated the HCM-induced endothelial migration (Fig. 2B). The effect of HCM on capillary-like tube structure stabilization was then examined. HCM clearly increased capillary-like tube formation, whereas isolinderalactone suppressed the HCM-induced formation of tube structures (Fig. 3A). Quantification of the tube length and branching points revealed the significant suppression of HCM-mediated tube formation by isolinderalactone (Fig. 3B and C).

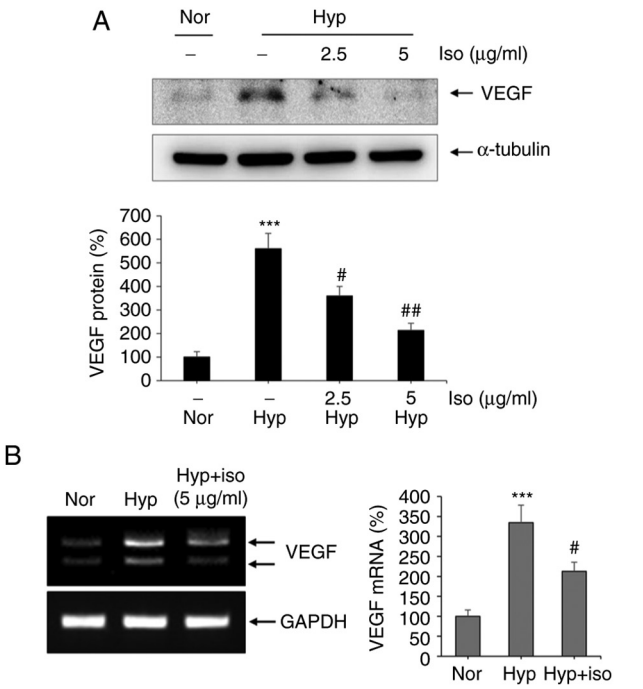


Figure 1. VEGF expression in U-87 glioblastoma cells. (A) VEGF protein level was measured by western blotting. Iso (2.5 or 5 $\mu$g/ml) was added to U-87 cultures grown in hypoxic conditions for 16 h (n=4). (B) Reverse transcription-PCR for VEGF was performed. Iso (5 $\mu$g/ml) was added to U-87 cells under hypoxic conditions for 16 h. The PCR fragments were separated by agarose gel electrophoresis (left). Quantified VEGF mRNA levels are presented in a graph (right) (n=5). $^{***}$P<0.001 vs. the Nor group; $^{\#}$P<0.05 and $^{\#\#}$P<0.01 vs. the Hyp group. VEGF, vascular endothelial growth factor; Iso, isolinderalactone; Nor, normoxic; Hyp, hypoxic.

*Isolinderalactone inhibits 3D angiogenic sprouting of tumor cell supernatants*. The anti-angiogenic effect of isolinderalactone was further examined in a 3D microfluidic device after the application of interstitial flow using glioblastoma CM (Fig. 4A). Angiogenic sprout growth was observed following HCM stimulation, and the addition of isolinderalactone to the cell culture inhibited sprout formation (Fig. 4B). Immunofluorescence staining of the HBMECs with anti-VE-cadherin (green) and anti-F-actin (red) antibodies showed that sprout length was significantly increased in the HCM-treated group, and the HCM-induced increase in sprout length was significantly decreased by isolinderalactone (Fig. 4C and D). However, sprout diameter did not differ among the groups (Fig. 4E).

*Isolinderalactone suppresses tumor cell supernatant-mediated in vivo angiogenesis*. To evaluate whether U-87 cell CM induces *in vivo* angiogenesis, which is inhibited by isolinderalactone, an *in vivo* mouse Matrigel plug assay was performed (Fig. 5). Mice were subcutaneously injected with Matrigel containing either NCM or HCM. Isolinderalactone treatment of mice with HCM was initiated after 24 h (Fig. 5A). HCM strongly increased angiogenic activity in the Matrigel plug, which was notably suppressed by isolinderalactone (Fig. 5B). The Matrigel with HCM had a significantly increased hemoglobin concentration compared with that in the Matrigel with NCM, and the hemoglobin concentration in the isolinderalactone-injected HCM group was significantly lower compared with that in the untreated HCM group (Fig. 5C).

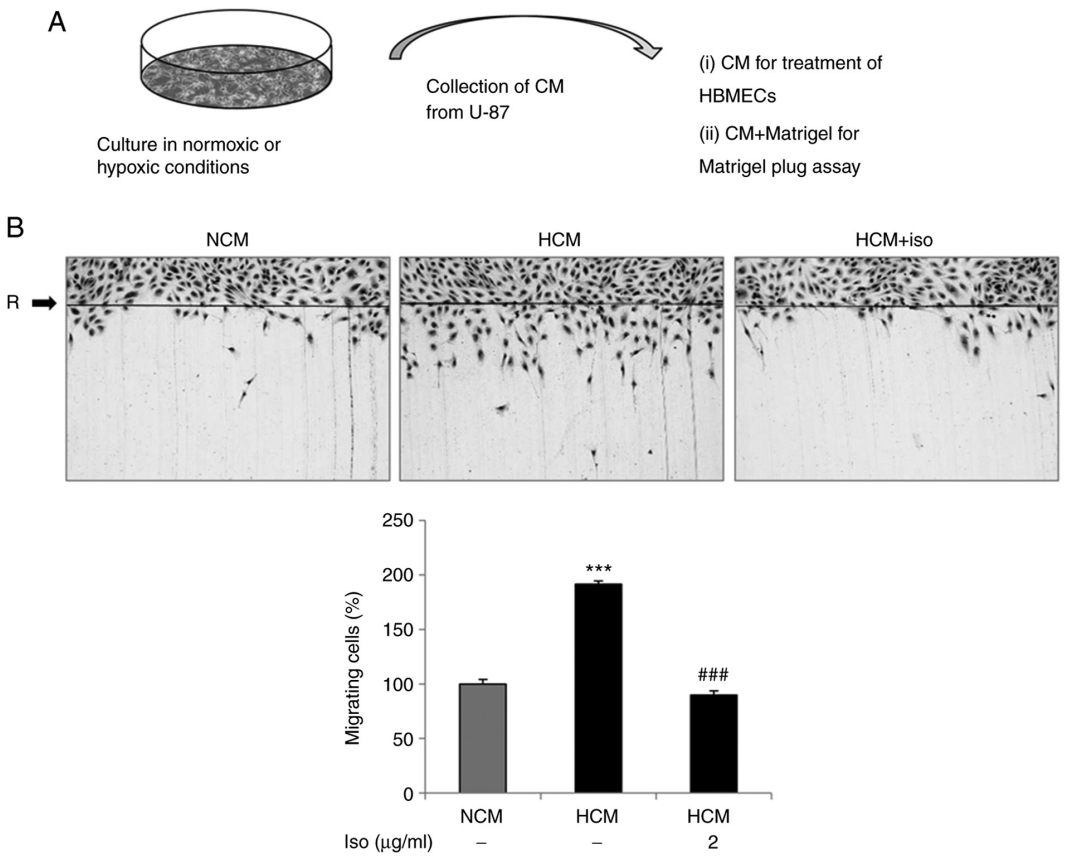


Figure 2. Iso suppresses HCM-mediated endothelial migration. (A) Illustration of CM preparation and use. NCM and HCM were each collected, concentrated and used for further experiments. (B) HBMECs were treated with CM from U-87 cells for 16 h, and an endothelial cell migration assay was performed (n=12). Iso (2 $\mu$g/ml) was added to cells grown in HCM. Magnification, x40. $^{***}$P<0.001 vs. the NCM group; $^{###}$P<0.001 vs. the HCM group. Iso, isolinderalactone; CM, conditioned medium; NCM, CM from normoxic U-87 cells; HCM, CM from hypoxic U-87 cells; HBMECs, human brain microvascular endothelial cells; R, reference line.

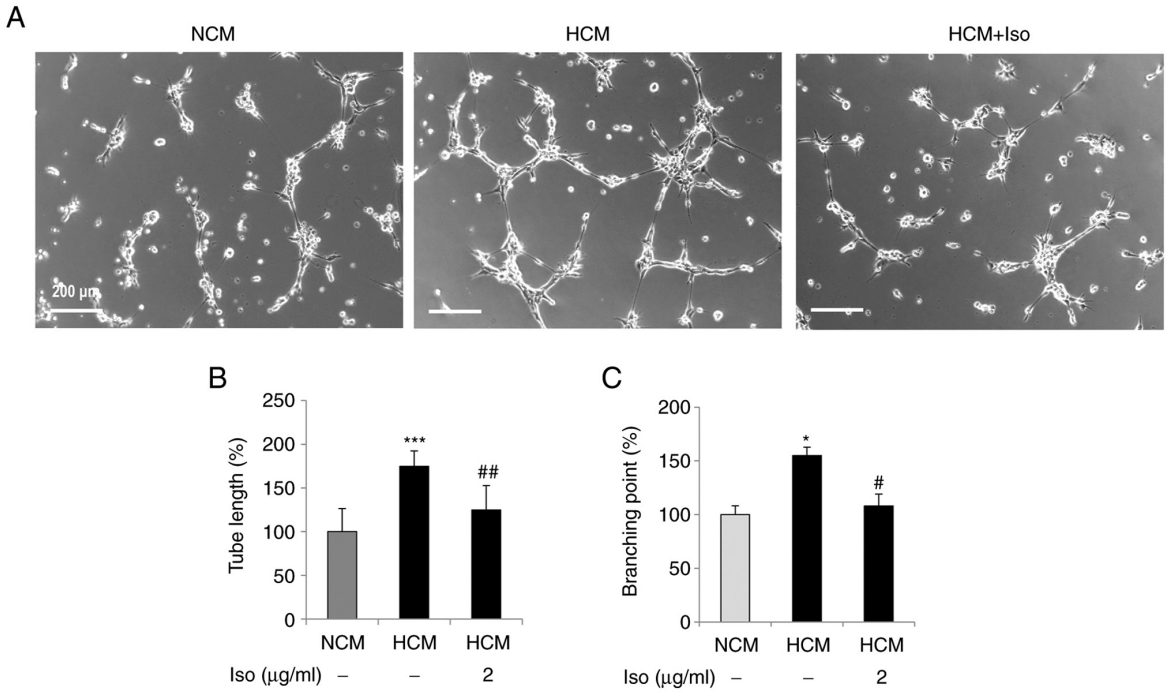


Figure 3. Iso reduces HCM-mediated tube formation. (A) Human brain microvascular endothelial cells were plated on growth factor-reduced Matrigel, and tube formation was observed at 7 h. HCM promoted tube formation and iso (2 $\mu$g/ml) attenuated the HCM-induced tube formation. Magnification, x100. Scale bar=200 $\mu$m. (B) Tube length and (C) branching points (>3) were quantified using iSolution full image analysis software (n=6-8). $^{*}$P<0.05 and $^{***}$P<0.001 vs. the NCM group; $^{\#}$P<0.05 and $^{\#\#}$P<0.01 vs. the HCM group. Iso, isolinderalactone; HCM, conditioned medium from hypoxic U-87 cells; NCM, conditioned medium from normoxic U-87 cells.

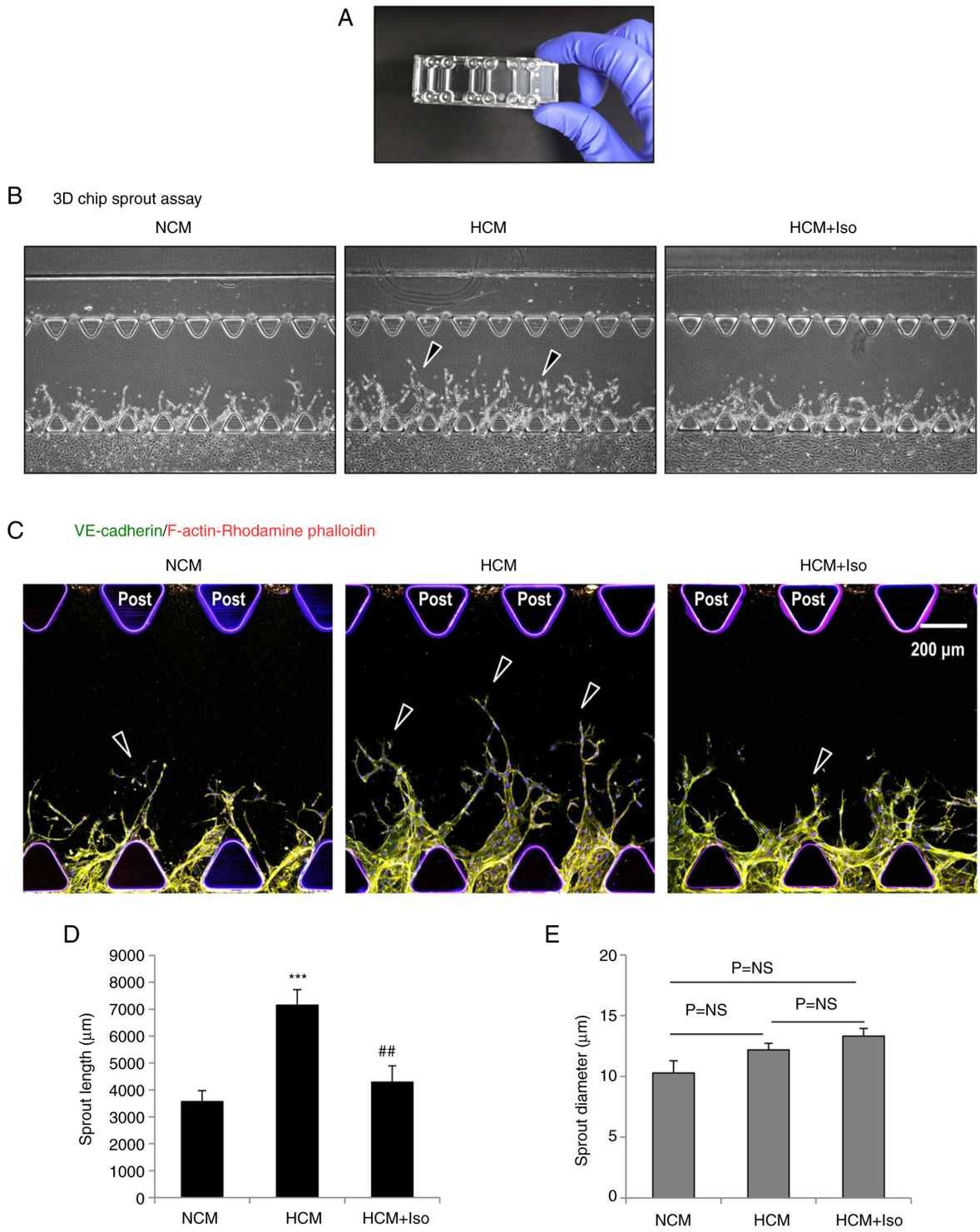


Figure 4. 3D angiogenic sprouting in a microfluidic device with interstitial flow. (A) A 3D chip device was used. (B) 3D phase-contrast images of HBMECs in the chip device were captured. NCM or HCM was added to the medium channel 1 day after cell seeding and were supplied to the HBMECs for 7 days. Iso (2 $\mu$g/ml) was added to the medium channel for 2 days prior to sprout fixation. Arrowheads indicate sprout morphology. Magnification, x40. (C) Immunofluorescence staining of the sprouts. On day 8 after cell seeding, the microvessels were fixed and stained for VE-cadherin (green) or F-actin (red). Confocal images show z-stack images of the angiogenic sprouts (arrowheads). Nuclei are stained with DAPI (blue). Magnification, x50; scale bar=200 $\mu$m. (D) Quantification of sprout length and (E) sprout diameter. $^{***}$P<0.001 vs. the NCM group. $^{\#\#}$P<0.01 vs. the HCM group. At least three or four randomly selected fields from each experiment were analyzed over three independent experiments. HBMECs, human brain microvascular endothelial cells; HCM, conditioned medium from hypoxic U-87 cells; NCM, conditioned medium from normoxic U-87 cells; iso, isolinderalactone; NS, not significant.

## Discussion

GBM is the most frequently occurring malignant primary brain tumor in adults (11). It is categorized as a grade IV astrocytoma in the World Health Organization classification and is the most aggressive tumor of the central nervous system (28). A common characteristic of GBMs is the high degree of tumor vascularization with extensive

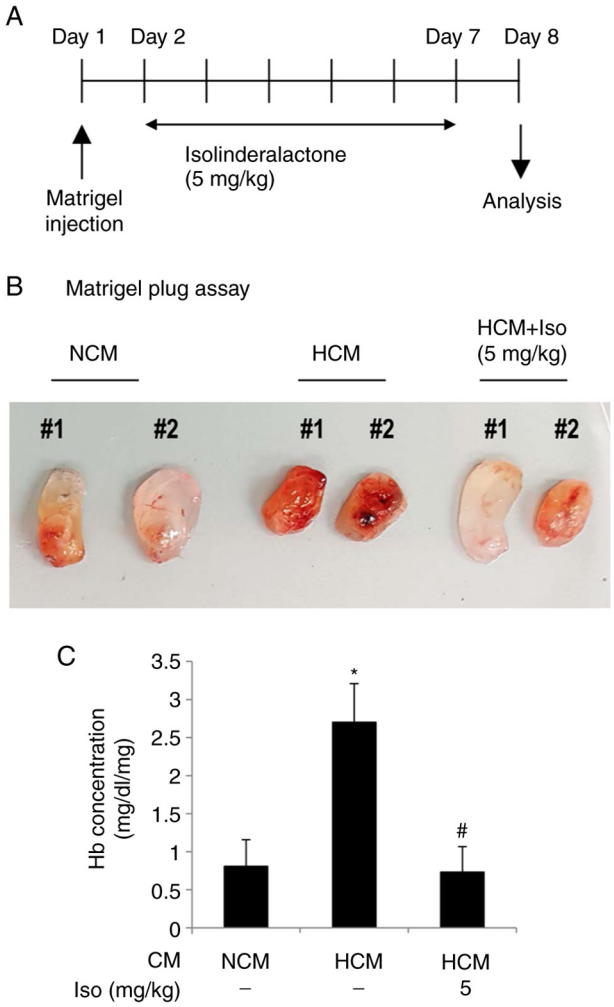


Figure 5. Iso inhibits HCM-mediated angiogenesis in an *in vivo* Matrigel plug assay. (A) Schematic illustration of Matrigel injection and isolinderalactone treatment. Matrigel with NCM or HCM was injected subcutaneously into mice, and the mice were treated with DMSO or isolinderalactone (5 mg/kg/day) by intraperitoneal injection for 6 days, starting 1 day after Matrigel injection. (B) Matrigel plugs were excised and images were captured on day 8. (C) Quantification of the formation of functional vasculature by Hb assay. Data are presented as the mean ± SEM. NCM (n=4), HCM + DMSO (n=6) and HCM + iso (n=6). $^{*}$P<0.05 vs. the NCM group; $^{\#}$P<0.01 vs. the HCM group. Iso, isolinderalactone; HCM, conditioned medium from hypoxic U-87 cells; NCM, conditioned medium from normoxic U-87 cells; Hb, hemoglobin.

angiogenesis and abnormal vessels. GBMs show remarkable endothelial proliferation, convoluted vessels with a variable diameter, reduced pericyte coverage and thickened basement membranes (18,19). Abnormal GBM vascularization is mainly due to the upregulation of angiogenic factors, including VEGF, which is an essential growth factor for vascular endothelial cells (18). Angiogenesis involves multiple steps: Signaling from ischemic tissues or hypoxic solid tumors activates quiescent endothelial cells, which degrade the basement membrane and extracellular matrix. The endothelial cells proliferate, migrate into the connective tissue and move toward the source of angiogenic stimuli. The formation of lumen formation, tubular sprouts and new basement membrane occurs, pericytes are recruited and functional vascular networks are formed. These angiogenic processes are tightly regulated by angiogenic and anti-angiogenic factors (29).

Anti-angiogenic therapy using bevacizumab, a humanized monoclonal antibody targeting VEGF, is the most studied anti-angiogenic treatment and shows the most promising results against tumor progression (30). However, clinical trials of bevacizumab have not demonstrated any extension of overall survival, although the drug appears to prolong progression-free survival and improve the quality of life (30). It is hypothesized that the development of resistance to anti-angiogenic therapy is based on the upregulation of angiogenic or pro-angiogenic factors other than VEGF. Angiogenic cytokines such as hepatocyte growth factor, FGF-2, platelet-derived growth factor, angiopoietins and interleukin-8 are upregulated in GBM (31-34). A study reported that the combined blockade of VEGF, angiopoietin-2 (Ang-2) and programmed cell death protein-1 increased the survival of GBM-bearing mice compared with that of GCM-bearing mice in which only VEGF or Ang-2 was blocked (35). Our previous study showed that isolinderalactone inhibited the VEGF expression pathway in GBMs under hypoxia and VEGF-induced angiogenesis (10). Moreover, the present study demonstrated that isolinderalactone successfully decreased the angiogenesis induced by hypoxic U-87 culture supernatant *in vitro* and *in vivo*. Notably, isolinderalactone reduced the sprout formation of HBMECs in a 3D microfluidic device after the application of interstitial flow using CM obtained from hypoxic U-87 cells. We hypothesize that the CM obtained from tumor cells contains numerous pro-angiogenic factors secreted by the cells, including VEGF, which thereby stimulate angiogenesis, and isolinderalactone can efficiently suppress this process.

The present study has certain limitations. First, the anti-angiogenic mechanism of isolinderalactone during HCM-mediated angiogenesis was not explored. Although HCM was used instead of recombinant VEGF, the activation of VEGFR2 in the HBMECs may be the target of isolinderalactone, as observed in our previous study (10). Further study is required to elucidate the mechanism. In addition, the constituents of the HCM were did not analyzed and the effective proteins or components with angiogenic activity were not identified. In addition to angiogenic cytokines, microRNA-containing extracellular vesicles, and non-coding RNAs can contribute to tumor angiogenesis (36,37). Thus, further research is necessary to identify such proteins or components. Another limitation of the present study is that only one GBM cell line was utilized. Therefore, the findings may not extend to all types of GBM. Isolinderalactone may have potential as an inhibitor of GBM angiogenesis, but confirmation of its general effectiveness should be explored in further investigations. In summary, the present study demonstrated that the supernatants of GBM cells cultured under hypoxic conditions stimulate angiogenesis, which is successfully inhibited by isolinderalactone. These findings indicate that isolinderalactone may have the potential to be developed as an anti-angiogenic medicine for GBM treatment.

**Acknowledgements**

Not applicable.

**Funding**

The current study was supported by a National Research Foundation of Korea grant funded by the Korea government (grant no. 2020R1A2C1012564).

**Availability of data and materials**

The datasets used and/or analyzed during the current study are available from the corresponding author on reasonable request.

**Authors' contributions**

SYL and HKS participated in the study design. JHP, KHC and HK conducted the experiments. SYL performed the data analysis. SYL and HKS wrote or contributed to the writing of the manuscript. SYL and HKS confirm the authenticity of all the raw data. All authors read and approved the final manuscript.

**Ethics approval and consent to participate**

Not applicable.

**Patient consent for publication**

Not applicable.

**Competing interests**

The authors declare that they have no competing interests.

**References**

1. Kobayashi W, Miyase T, Sano M, Umehara K, Warashina T and Noguchi H: Prolyl endopeptidase inhibitors from the roots of *Lindera* strychnifolia F. Vill. Biol Pharm Bull 25: 1049-1052, 2002.
2. Gan LS, Zheng YL, Mo JX, Liu X, Li XH and Zhou CX: Sesquiterpene lactones from the root tubers of *Lindera aggregata*. J Nat Prod 72: 1497-1501, 2009.
3. Ohno T, Takemura G, Murata I, Kagawa T, Akao S, Minatoguchi S, Fujiwara T and Fujiwara H: Water extract of the root of *Lindera* strychnifolia slows down the progression of diabetic nephropathy in db/db mice. Life Sci 77: 1391-1403, 2005.
4. Wang F, Gao Y, Zhang L and Liu JK: Bi-linderone, a highly modified methyl-linderone dimer from *Lindera aggregata* with activity toward improvement of insulin sensitivity in vitro. Org Lett 12: 2354-2357, 2010.
5. Chang WA, Lin ES, Tsai MJ, Huang MS and Kuo PL: Isolinderalactone inhibits proliferation of A549 human non-small cell lung cancer cells by arresting the cell cycle at the G0/G1 phase and inducing a Fas receptor and soluble Fas ligand-mediated apoptotic pathway. Mol Med Rep 9: 1653-1659, 2014.
6. Yen MC, Shih YC, Hsu YL, Lin ES, Lin YS, Tsai EM, Ho YW, Hou MF and Kuo PL: Isolinderalactone enhances the inhibition of SOCS3 on STAT3 activity by decreasing miR-30c in breast cancer. Oncol Rep 35: 1356-1364, 2016.
7. Chuang CH, Wang LY, Wong YM and Lin ES: Anti-metastatic effects of isolinderalactone via the inhibition of MMP-2 and up regulation of NM23-H1 expression in human lung cancer A549 cells. Oncol Lett 15: 4690-4696, 2018.
8. Rajina S, Kim WJ, Shim JH, Chun KS, Joo SH, Shin HK, Lee SY and Choi JS: Isolinderalactone induces cell death via mitochondrial superoxide- and STAT3-mediated pathways in human ovarian cancer cells. Int J Mol Sci 21: 7530, 2020.
9. Hwang JY, Park JH, Kim MJ, Kim WJ, Ha KT, Choi BT, Lee SY and Shin HK: Isolinderalactone regulates the BCL-2/caspase-3/PARP pathway and suppresses tumor growth in a human glioblastoma multiforme xenograft mouse model. Cancer Lett 443: 25-33, 2019.
10. Park JH, Kim MJ, Kim WJ, Kwon KD, Ha KT, Choi BT, Lee SY and Shin HK: Isolinderalactone suppresses human glioblastoma growth and angiogenic activity in 3D microfluidic chip and in vivo mouse models. Cancer Lett 478: 71-81, 2020.
11. Camelo-Piragua S and Kesari S: Further understanding of the pathology of glioma: Implications for the clinic. Expert Rev Neurother 16: 1055-1065, 2016.
12. Stupp R, Mason WP, van den Bent MJ, Weller M, Fisher B, Taphoorn MJ, Belanger K, Brandes AA, Marosi C, Bogdahn U, *et al*: Radiotherapy plus concomitant and adjuvant temozolomide for glioblastoma. N Engl J Med 352: 987-996, 2005.
13. Stupp R, Hegi ME, Mason WP, van den Bent MJ, Taphoorn MJ, Janzer RC, Ludwin SK, Allgeier A, Fisher B, Belanger K, *et al*: Effects of radiotherapy with concomitant and adjuvant temozolomide versus radiotherapy alone on survival in glioblastoma in a randomised phase III study: 5-Year analysis of the EORTC-NCIC trial. Lancet Oncol 10: 459-466, 2009.
14. Wen PY and Kesari S: Malignant gliomas in adults. N Engl J Med 359: 492-507, 2008.
15. Norden AD, Drappatz J and Wen PY: Antiangiogenic therapies for high-grade glioma. Nat Rev Neurol 5: 610-620, 2009.
16. Ribatti D and Pezzella F: Vascular co-option and other alternative modalities of growth of tumor vasculature in glioblastoma. Front Oncol 12: 874554, 2022.
17. Hanahan D and Folkman J: Patterns and emerging mechanisms of the angiogenic switch during tumorigenesis. Cell 86: 353-364, 1996.
18. Plate KH and Mennel HD: Vascular morphology and angiogenesis in glial tumors. Exp Toxicol Pathol 47: 89-94, 1995.
19. Chi AS, Sorensen AG, Jain RK and Batchelor TT: Angiogenesis as a therapeutic target in malignant gliomas. Oncologist 14: 621-636, 2009.
20. Sisakht AK, Malekan M, Ghobadinezhad F, Firouzabadi SNM, Jafari A, Mirazimi SMA, Abadi B, Shafabakhsh R and Mirzaei H: Cellular conversations in glioblastoma progression, diagnosis and treatment. Cell Mol Neurobiol: Apr 11, 2022 (Epub ahead of print).
21. Plate KH, Breier G, Weich HA and Risau W: Vascular endothelial growth factor is a potential tumour angiogenesis factor in human gliomas in vivo. Nature 359: 845-848, 1992.
22. Gilbertson RJ and Rich JN: Making a tumour's bed: Glioblastoma stem cells and the vascular niche. Nat Rev Cancer 7: 733-736, 2007.
23. Nomura M, Yamagishi S, Harada S, Hayashi Y, Yamashima T, Yamashita J and Yamamoto H: Possible participation of autocrine and paracrine vascular endothelial growth factors in hypoxia-induced proliferation of endothelial cells and pericytes. J Biol Chem 270: 28316-28324, 1995.
24. Yang J, Kim WJ, Jun HO, Lee EJ, Lee KW, Jeong JY and Lee SW: Hypoxia-induced fibroblast growth factor 11 stimulates capillary-like endothelial tube formation. Oncol Rep 34: 2745-2751, 2015.
25. Lee SW, Kim WJ, Choi YK, Song HS, Son MJ, Gelman IH, Kim YJ and Kim KW: SSeCKS regulates angiogenesis and tight junction formation in blood-brain barrier. Nat Med 9: 900-906, 2003.
26. van Duinen V, Zhu D, Ramakers C, van Zonneveld AJ, Vulto P and Hankemeier T: Perfused 3D angiogenic sprouting in a high-throughput in vitro platform. Angiogenesis 22: 157-165, 2019.
27. Folkman J: Angiogenesis: An organizing principle for drug discovery? Nat Rev Drug Discov 6: 273-286, 2007.
28. Louis DN, Perry A, Wesseling P, Brat DJ, Cree IA, Figarella-Branger D, Hawkins C, Ng HK, Pfister SM, Reifenberger G, *et al*: The 2021 WHO classification of tumors of the central nervous system: A summary. Neuro Oncol 23: 1231-1251, 2021.
29. Holash J, Wiegand SJ and Yancopoulos GD: New model of tumor angiogenesis: Dynamic balance between vessel regression and growth mediated by angiopoietins and VEGF. Oncogene 18: 5356-5362, 1999.
30. Fine HA: Bevacizumab in glioblastoma-still much to learn. N Engl J Med 370: 764-765, 2014.

31. Schmidt NO, Westphal M, Hagel C, Ergün S, Stavrou D, Rosen EM and Lamszus K: Levels of vascular endothelial growth factor, hepatocyte growth factor/scatter factor and basic fibroblast growth factor in human gliomas and their relation to angiogenesis. Int J Cancer 84: 10-18, 1999.
32. Reiss Y, Machein MR and Plate KH: The role of angiopoietins during angiogenesis in gliomas. Brain Pathol 15: 311-317, 2005.
33. Brat DJ, Bellail AC and Van Meir EG: The role of interleukin-8 and its receptors in gliomagenesis and tumoral angiogenesis. Neuro Oncol 7: 122-133, 2005.
34. Shih AH and Holland EC: Platelet-derived growth factor (PDGF) and glial tumorigenesis. Cancer Lett 232: 139-147, 2006.
35. Di Tacchio M, Macas J, Weissenberger J, Sommer K, Bähr O, Steinbach JP, Senft C, Seifert V, Glas M, Herrlinger U, *et al*: Tumor vessel normalization, immunostimulatory reprogramming, and improved survival in glioblastoma with combined inhibition of PD-1, angiopoietin-2, and VEGF. Cancer Immunol Res 7: 1910-1927, 2019.
36. Lucero R, Zappulli V, Sammarco A, Murillo OD, Cheah PS, Srinivasan S, Tai E, Ting DT, Wei Z, Roth ME, *et al*: Glioma-derived miRNA-containing extracellular vesicles induce angiogenesis by reprogramming brain endothelial cells. Cell Rep 30: 2065-2074.e4, 2020.
37. Li D, Zhang Z, Xia C, Niu C and Zhou W: Non-coding RNAs in glioma microenvironment and angiogenesis. Front Mol Neurosci 14: 763610, 2021.